Correlated singlet phase in the one-dimensional Hubbard-Holstein model

Sahinur Reja,[1,2] Sudhakar Yarlagadda,[1] and Peter B. Littlewood[2,3,4]

[1]*CAMCS and TCMP Div., Saha Institute of Nuclear Physics, Kolkata, India*
[2]*Cavendish Lab, Univ. of Cambridge, Cambridge, United Kingdom*
[3]*Argonne National Laboratory, Argonne, Illinois 60439, USA*
[4]*University of Chicago, James Franck Institute, Chicago, Illinois 60637, USA*

We show that a nearest-neighbor singlet phase results (from an effective Hamiltonian) for the one-dimensional Hubbard-Holstein model in the regime of strong electron-electron and electron-phonon interactions and under nonadiabatic conditions ($t/\omega_0 \leqslant 1$). By mapping the system of nearest-neighbor singlets at a filling N_p/N onto a hard-core-boson (HCB) t-V model at a filling $N_p/(N - N_p)$, we demonstrate explicitly that superfluidity and charge density wave (CDW) occur mutually exclusively with the diagonal long range order manifesting itself only at one-third filling. Furthermore, we also show that the Bose-Einstein condensate (BEC) occupation number n_0 for the singlet phase, similar to the n_0 for a HCB tight binding model, scales as $\sqrt{N}$; however, the coefficient of $\sqrt{N}$ in the n_0 for the interacting singlet phase is numerically demonstrated to be smaller.

I. INTRODUCTION

The study of coexistence and competition between diagonal long range orders [such as charge density wave (CDW) and spin density wave (SDW)] and off-diagonal long range orders (such as superfluid and superconducting states) in electronic phases is a subject of immense ongoing focus. Of particular interest is the coexistence of CDW and superconductivity/superfluidity in layered dichalogenides (e.g., 2H-TaSe$_2$, 2H-TaS$_2$, and NbSe$_2$),[1] helium-4,[2] bismuthates (e.g., BaBiO$_3$ doped with K or P),[3] quasi-one-dimensional trichalcogenide NbSe$_3$,[4] and doped spin ladder cuprate Sr$_{14}$Cu$_{24}$O$_{41}$,[5] quarter-filled organic materials,[6,7] noniron based pnictides (e.g., SrPt$_2$As$_2$),[8] etc.

Systems with more than one type of interaction typically manifest a variety of phases of which some cooperate and some compete. A wealth of materials show evidence of strong electron-phonon (e-ph) interactions besides the ubiquitous electron-electron (e-e) interactions. For instance, transition metal oxides such as cuprates[9,10] and manganites[11–13] and molecular solids such as fullerides[14] indicate strong e-ph coupling. The interplay of e-e and e-ph interactions in these correlated systems leads to coexistence of or competition between various phases such as superconductivity, CDW, SDW, etc.

An archetypal model for understanding the co-occurring effects of e-e and e-ph interactions is the following well known Hubbard-Holstein model (HHM):[15]

$$H_{hh} = -t \sum_{j\sigma} (c_{j+1\sigma}^\dagger c_{j\sigma} + \text{H.c.}) + \omega_0 \sum_j a_j^\dagger a_j$$
$$+ g\omega_0 \sum_{j\sigma} n_{j\sigma}(a_j + a_j^\dagger) + U \sum_j n_{j\uparrow} n_{j\downarrow}, \quad (1)$$

where $c_{j\sigma}^\dagger$ is the fermionic creation operator for itinerant spin-σ electrons with hopping integral t, and number operator $n_{j\sigma} \equiv c_{j\sigma}^\dagger c_{j\sigma}$, $a_j^\dagger$ is the corresponding bosonic creation operator characterized by a dispersionless phonon frequency

ω_0, with U and g representing the strengths of onsite e-e and e-ph interactions respectively.

To understand the interplay between the e-e and e-ph interactions, the Hubbard-Holstein model has been extensively studied (in one, two, and infinite dimensions and at various fillings) by employing various approaches such as exact diagonalization,[16–18] density matrix renormalization group (DMRG),[19,20] quantum Monte Carlo (QMC),[21–26] semi-analytical slave boson approximations,[27–31] dynamical mean field theory (DMFT),[32–40] large-N expansion,[41] variational methods based on Lang-Firsov transformation,[42,43] Gutzwiller approximation,[44,45] and cluster approximation.[46]

In our earlier work,[15] in the regimes of strong Coulomb interaction and strong e-ph coupling, we derived an effective Hamiltonian using a controlled analytic approach that takes into account dynamical quantum phonons. We solved this effective Hamiltonian numerically for finite chains and presented a phase diagram for the one-dimensional Hubbard-Holstein model at quarter filling. It was shown in Ref. 15 that while the e-e interaction produces nearest-neighbor (NN) spin antiferromagnetic (AF) interactions which encourage singlet formation, the e-ph interaction generates NN repulsion which is expected to promote CDW order. It was also shown that a correlated NN singlet phase occurs (at quarter-filling) and that it carries a signature of a CDW. In this paper, we demonstrate that the correlated singlet phase occurs at other fractions as well and analyze its nature. Our main result is the demonstration that the NN spin AF and NN repulsive interactions compete (instead of cooperate) to produce mutually exclusive (rather than coexisting) superfluid and CDW phases in the NN singlet phase. We show that the NN singlets manifest superfluidity (and no CDW) at all fillings that are less than one-half but not equal to one-third and a CDW state (and no superfluidity) at one-third filling. Using a modified Lanczos method[15,47] and a newly developed world-line quantum Monte Carlo (WQMC) method, we show that the singlet phase has no Bose-Einstein condensate (BEC) fraction.

In the past, superconductivity due to onsite pairing has been a focus of a number of studies.[48–50] Here we are

interested in a different situation, namely, NN singlets. Earlier a t-J-V model (involving bipolarons that are NN singlets) was introduced in Ref. 51. This t-J-V model[51] [that does not include the next-nearest-neighbor hopping terms but discusses them qualitatively] is similar to our effective Hamiltonian of Eq. (9) and can be regarded as a useful precedent and an endorsement of Eq. (9).

The paper is organized as follows: In Sec. II we briefly derive the effective Hamiltonian (that goes beyond the t-J model approximation of the Hubbard model by including the additional three site residue[52–54]) and explain the various interaction terms and hopping terms. We also point out that the correlated singlet phase occurs at not only quarter-filling but also at other fillings. In Sec. III, we show that the correlated singlet phase can be represented by a hard-core-boson (HCB) t-V_1-V_2 model. Next, in Sec. IV we discuss the possibility of formation of a CDW by mapping the t-V_1-V_2 model onto the well understood t-V model. In Sec. V, we obtain the superfluid density (in the thermodynamic limit) at different filling fractions by using finite size scaling. In Sec. VI, we analyze the BEC occupation number at various densities by employing the modified Lanczos method and a newly developed WQMC method. We close with concluding remarks in Sec. VII.

II. EFFECTIVE HHM HAMILTONIAN

We briefly outline below the procedure to get the effective Hubbard-Holstein Hamiltonian (with more details being provided in Ref. 15). Although we obtain the effective Hamiltonian here in one dimension only, our approach is easily extendable to higher dimensions as well. We first carry out the Lang-Firsov (LF) transformation[55] $H_{hh}^{LF} = e^T H_{hh} e^{-T}$ where $T = -g \sum_{j\sigma} n_{j\sigma}(a_j - a_j^\dagger)$ and get the following LF transformed Hamiltonian:

$$H_{hh}^{LF} = -t \sum_{j\sigma}(X_{j+1}^\dagger c_{j+1\sigma}^\dagger c_{j\sigma} X_j + \text{H.c.}) + \omega_0 \sum_j a_j^\dagger a_j$$
$$- g^2\omega_0 \sum_j n_j + (U - 2g^2\omega_0)\sum_j n_{j\uparrow} n_{j\downarrow}, \quad (2)$$

where $X_j = e^{g(a_j - a_j^\dagger)}$ and $n_j = n_{j\uparrow} + n_{j\downarrow}$. Next, we express as follows our LF transformed Hamiltonian in terms of the composite fermionic operator $d_{j\sigma}^\dagger \equiv c_{j\sigma}^\dagger X_j^\dagger$:

$$H_{hh}^{LF} = -t \sum_{j\sigma}(d_{j+1\sigma}^\dagger d_{j\sigma} + \text{H.c.}) + \omega_0 \sum_j a_j^\dagger a_j$$
$$+ (U - 2g^2\omega_0)\sum_j n_{j\uparrow}^d n_{j\downarrow}^d - g^2\omega_0 \sum_j \left(n_{j\uparrow}^d + n_{j\downarrow}^d\right), \quad (3)$$

where $n_{j\sigma}^d = d_{j\sigma}^\dagger d_{j\sigma}$. On dropping the last term, which is a constant polaronic energy, we recognize that Eq. (3) essentially represents the Hubbard model for composite fermions with Hubbard interaction $U_{\text{eff}} = (U - 2g^2\omega_0)$. In the limit of large U_{eff}/t, using standard treatment involving a canonical transformation, we get the following effective Hamiltonian

written to second order in the small parameter t/U_{eff} :[52–54]

$$H_{t\text{-}J\text{-}t_3} = P_s\Bigg[-t\sum_{j\sigma}(d_{j+1\sigma}^\dagger d_{j\sigma} + \text{H.c.}) + \omega_0 \sum_j a_j^\dagger a_j$$
$$+ J\sum_j \left(\vec{S}_j \cdot \vec{S}_{j+1} - \frac{n_j^d n_{j+1}^d}{4}\right)$$
$$+ t_3 \sum_{j\sigma}[d_{j\bar\sigma}^\dagger d_{j+1\sigma} d_{j-1\sigma}^\dagger d_{j\bar\sigma} + \text{H.c.}]$$
$$- t_3 \sum_{j\sigma}[d_{j\sigma}^\dagger d_{j+1\sigma} d_{j-1\bar\sigma}^\dagger d_{j\bar\sigma} + \text{H.c.}]\Bigg]P_s, \quad (4)$$

where $n_j^d = n_{j\uparrow}^d + n_{j\downarrow}^d$, $J = \frac{4t^2}{U - 2g^2\omega_0}$, $t_3 = J/4$, $\vec{S}_i$ is the spin operator for a spin $1/2$ fermion at site i, and P_s is the single-occupancy-subspace projection operator. Furthermore, the last two terms with coefficient t_3 ($=J/4$) are the three site terms which when omitted from the above Hamiltonian $H_{t\text{-}J\text{-}t_3}$ yield the well-known t-J Hamiltonian (for the composite fermionic operators $d_{j\sigma}$).

The effective t-J-t_3 Hamiltonian, given in Eq. (4), can be rewritten in terms of the original fermionic operators $c_{j\sigma}$ as

$$H_{t\text{-}J\text{-}t_3} = H_0 + H_1, \quad (5)$$

where

$$H_0 = -te^{-g^2}\sum_{j\sigma} P_s(c_{j+1\sigma}^\dagger c_{j\sigma} + \text{H.c.})P_s + \omega_0 \sum_j a_j^\dagger a_j$$
$$+ J\sum_j P_s\left(\vec{S}_j \cdot \vec{S}_{j+1} - \frac{n_j n_{j+1}}{4}\right)P_s$$
$$+ \frac{Je^{-g^2}}{4}\sum_{j\sigma} P_s[c_{j\bar\sigma}^\dagger c_{j+1\sigma} c_{j-1\sigma}^\dagger c_{j\bar\sigma} + \text{H.c.}]P_s$$
$$- \frac{Je^{-g^2}}{4}\sum_{j\sigma} P_s[c_{j\sigma}^\dagger c_{j+1\sigma} c_{j-1\bar\sigma}^\dagger c_{j\bar\sigma} + \text{H.c.}]P_s, \quad (6)$$

and

$$H_1 = -te^{-g^2}\sum_{j\sigma} P_s[c_{j+1\sigma}^\dagger c_{j\sigma}(Y_+^{j\dagger}Y_-^j - 1) + \text{H.c.}]P_s. \quad (7)$$

In the above equation, we have separated the $H_{t\text{-}J\text{-}t_3}$ Hamiltonian into (i) an electronic part H_0 which is essentially a modified t-J-t_3 Hamiltonian containing a NN hopping with a reduced amplitude (te^{-g^2}), electronic interaction terms with the same interaction strength J, three site terms with reduced amplitude $Je^{-g^2}/4$, and no electron-phonon interaction, and (ii) the remaining perturbative part H_1 which corresponds to the composite fermion terms containing the e-ph interaction with $Y_\pm^j \equiv e^{\pm g(a_{j+1} - a_j)}$. Furthermore, since $J/4 \ll t$, we have ignored the following term in H_1:

$$P_s\Bigg[\frac{Je^{-g^2}}{4}\sum_{j\sigma}[c_{j\bar\sigma}^\dagger c_{j+1\sigma} c_{j-1\sigma}^\dagger c_{j\bar\sigma}(Z_+^{j\dagger}Z_-^j - 1) + \text{H.c.}]$$
$$- \frac{Je^{-g^2}}{4}\sum_{j\sigma}[c_{j\sigma}^\dagger c_{j+1\sigma} c_{j-1\bar\sigma}^\dagger c_{j\bar\sigma}(Z_+^{j\dagger}Z_-^j - 1) + \text{H.c.}]\Bigg]P_s, \quad (8)$$

where $Z_\pm^j \equiv e^{\pm g(a_{j-1} - a_{j+1})}$.

After carrying out perturbation theory to second-order (as outlined in Ref. 15 and Appendix A), with $t/(g\omega_0)$ as the small parameter,[56] we get the following effective Hamiltonian:

$$H_{hh}^{\text{eff}} \cong -t_{\text{eff}}h_{t_1} + Jh_S - Vh_{nn} - t_2h_{\sigma\sigma}$$
$$- (t_2 + J_3)h_{\sigma\bar{\sigma}} + J_3h'_{\sigma\bar{\sigma}}, \quad (9)$$

where

$$h_{t_1} = \sum_{j\sigma} P_s(c^{\dagger}_{j+1\sigma}c_{j\sigma} + \text{H.c.})P_s, \quad (10)$$

$$h_S = \sum_j P_s\left(\vec{S}_j \cdot \vec{S}_{j+1} - \frac{1}{4}n_jn_{j+1}\right)P_s, \quad (11)$$

$$h_{nn} = \sum_{j\sigma} (1 - n_{j+1\bar{\sigma}})(1 - n_{j\bar{\sigma}})(n_{j\sigma} - n_{j+1\sigma})^2, \quad (12)$$

$$h_{\sigma\sigma} = \sum_{j\sigma} (1 - n_{j+1\bar{\sigma}})(1 - n_{j\bar{\sigma}})(1 - n_{j-1\bar{\sigma}})$$
$$\times [c^{\dagger}_{j+1\sigma}(1 - 2n_{j\sigma})c_{j-1\sigma} + \text{H.c.}], \quad (13)$$

$$h_{\sigma\bar{\sigma}} = \sum_{j\sigma} (1 - n_{j+1\bar{\sigma}})(1 - n_{j-1\sigma})$$
$$\times [c^{\dagger}_{j\sigma}c_{j+1\sigma}c^{\dagger}_{j-1\bar{\sigma}}c_{j\bar{\sigma}} + \text{H.c.}], \quad (14)$$

and

$$h'_{\sigma\bar{\sigma}} = \sum_{j\sigma} (1 - n_{j+1\bar{\sigma}})(1 - n_{j\sigma})(1 - n_{j-1\bar{\sigma}})$$
$$\times [c^{\dagger}_{j\bar{\sigma}}c_{j+1\sigma}c^{\dagger}_{j-1\sigma}c_{j\bar{\sigma}} + \text{H.c.}]. \quad (15)$$

The various coefficients are defined in terms of the system electron-phonon coupling g, the Hubbard interaction U, the hopping amplitude t, and the phonon frequency ω_0 as follows: $V \simeq t^2/2g^2\omega_0$, $J \equiv \frac{4t^2}{U-2g^2\omega_0}$, $t_{\text{eff}} \equiv te^{-g^2}$, $t_2 \simeq t^2e^{-g^2}/g^2\omega_0$, and $J_3 = Je^{-g^2}/4$. Here the kinetic energy (which is small compared to the interaction energy) has contributions from four hopping terms: $-t_{\text{eff}}h_{t_1}$ corresponding to NN hopping (with a reduced hopping integral $t_{\text{eff}} \equiv te^{-g^2}$), $-t_2h_{\sigma\sigma}$ representing NNN hopping (with double-hopping coefficient $t_2 \simeq t^2e^{-g^2}/g^2\omega_0$), $-(t_2 + J_3)h_{\sigma\bar{\sigma}}$ implying NN spin-pair $\sigma\bar{\sigma}$ hopping, and $J_3h'_{\sigma\bar{\sigma}}$ leading to NN spin-pair $\sigma\bar{\sigma}$ hopping and flipping to $\bar{\sigma}\sigma$; thus $h'_{\sigma\bar{\sigma}}$ acting on a singlet state produces another singlet state, but with a negative sign. The NN spin-spin interaction term Jh_S (with $J \equiv \frac{4t^2}{U-2g^2\omega_0}$) and the NN repulsion term $-Vh_{nn}$ (with $V \simeq t^2/2g^2\omega_0$) are the dominant terms in the effective Hamiltonian and compete to form a phase separated cluster at larger J (or smaller U/t at a fixed g and t/ω_0). As J/V decreases, the cluster breaks up to undergo a discontinuous transition to a correlated NN singlet phase as shown in the phase diagram [see Fig. 1(a)].[57] At even lower values of J/V, we get separated single spins (represented by isolated spin phase) with the transition at larger g being first order while at smaller g it is weakly first order and not continuous [due to the fact that the system transforms from a superfluid to a CDW, i.e., transition is between two phases of different symmetry].[15] *The prime objective of the current work is to characterize the correlated singlet state.*

We will now compare the physics related to our effective Hamiltonian, which accounts for various
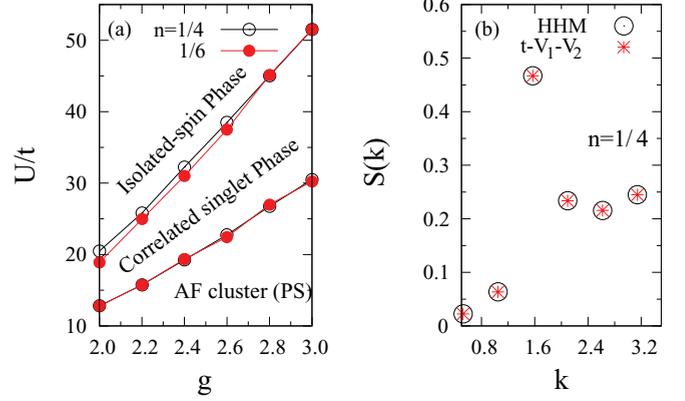
FIG. 1. (Color online) Plots obtained using modified Lanczos in a twelve-site system for $t/\omega_0 = 1$. Phase diagram in (a) depicts that the phase transition lines are close for both densities $n = 1/4$ and $n = 1/6$. Structure factor plots in (b) (drawn at $g = 2.2$ and $U/t = 17$) for the effective Hubbard-Holstein model (HHM) of Eq. (9) and the HCB t-V_1-V_2 model of Eq. (16) showing that the two models are equivalent.

fundamental processes involved in the kinetic and interaction terms, with the variational Lang-Firsov (LF) treatments reported.[30,31,38,43,45] As the degree of nonadiabaticity decreases, our NNN hopping term $-t_2h_{\sigma\sigma}$ contribution increases, effectively the hopping transport will be larger than that given by $-t_{\text{eff}}h_{t_1}$; these two hopping terms together can be regarded as producing a less than e^{-g^2} suppression of the hopping integral reported in earlier variational LF treatments. Furthermore, concerning the effect of including a large Hubbard U term in a Holstein model, we get the NN interaction $2V$ reduced to $2V - J/4$; thus, the mobility would be enhanced, which is consistent again with the earlier works using variational LF transformation.

III. t-V_1-V_2 HARD-CORE-BOSON (HCB) MODEL

In the rest of the paper we study the correlated singlet phase. No pair of singlets can share a common site. The closest two singlets can approach each other is to have one spin from each singlet be on adjacent sites. The singlets transport via two processes: (i) the NN spin-pair $\sigma\bar{\sigma}$ hopping given by the $h_{\sigma\bar{\sigma}}$ and $h'_{\sigma\bar{\sigma}}$ terms in Eq. (9), and (ii) a second order process involving breaking of a bound singlet state [with binding energy $E_B = -J + t^2/(g^2\omega_0)$] and hopping of the two constituent spins (of the singlet) to (a) neighboring sites in the same direction sequentially [yielding the term $-t_bh_{\sigma\bar{\sigma}}$ with $t_b \equiv t^2e^{-2g^2}/|E_B|$] or (b) neighboring sites in opposite direction and back [yielding the term $-t_bh_{nn}$]. We now make the important observation that a NN singlet can be represented as a HCB located at the center of the singlet. Thus the system of NN singlets in a periodic lattice is transformed into a system of HCB also in a periodic lattice with the same lattice constant a but with the whole lattice displaced by $a/2$. Then the effective Hamiltonian of the HCB system is the following t-V_1-V_2 model:

$$H_b = \sum_j [-T(b^{\dagger}_jb_{j+1} + \text{H.c.}) + V_1n_jn_{j+1} + V_2n_jn_{j+2}], \quad (16)$$

where b_j is the HCB destruction operator, $n_j = b_j^\dagger b_j$, $T \equiv (t_2 + 2J_3 + t_b)$, $V_1 = \infty$ (because two singlets cannot share a site), and $V_2 \simeq 2V - J/4$ [with $V_2/T > 10$ (i.e., $V_2/T \gg 1$) for parameter values in the singlet regime of our phase diagrams in Fig. 1(a)]. In the following we set $T = 1$. We corroborate our mapping of the effective HHM Hamiltonian H_{hh}^{eff} (for the singlet phase) onto the HCB Hamiltonian H_b by demonstrating in Fig. 1(b) that the static structure factor $S(k) \equiv \sum_l e^{ikl} W(l)$ for the HHM and HCB cases coincide when the correlation function $W(l) \equiv (1/N) \sum_j [\langle A_j A_{j+l} \rangle - \langle A_j \rangle \langle A_{j+l} \rangle]$ is defined through $A_j \equiv (S_j^+ S_{j+1}^- + \text{H.c.})$ for HHM and $A_j \equiv n_j$ for HCB.

It should be made clear that, for performing calculations, there is a distinct advantage of accessing bigger system sizes for the HCB system as compared to the HHM Hamiltonian. For instance calculations involving 8 HCB (equivalent to 8↑ and 8↓ electrons) on a 24 site lattice require

$$\binom{24}{8} = 735471$$

basis states in the occupation number representation and hence are certainly feasible using modified Lanczos method; on the other hand, using the same technique, one can barely deal with 8 electrons (4↑ and 4↓) on a 16 site lattice for the HHM Hamiltonian as it requires

$$\binom{16}{8} \times \binom{8}{4} = 900900$$

basis states. It is also of interest to note that representing a NN singlet by a HCB located at the center of the singlet, although has been done here for a one-dimensional system, can also be done in higher dimensional systems.

IV. CDW CORRELATIONS

The repulsive terms in the HCB Hamiltonian H_b indicate that a CDW is possible. We study the correlations by extending to our t-V_1-V_2 model the well documented WQMC approach for obtaining correlation functions and structure factor for the t-V model.[58] Plots of the structure factor in Fig. 2 show a peak at wave vector $Q = 2\pi n$ suggesting a CDW. However (as shown in Fig. 2), only at filling $n = 1/3$, where the structure factor peak is approximately that for the strong CDW case corresponding to $V_2 \to \infty$, can we assert that CDW occurs. Specifically at $n = 1/3$ and for $V_2 > 10$, the $W(l)$ has a simple structure [i.e., $W(l) \approx 1/3 - 1/3 \times 1/3 = 2/9$ when l is a multiple of 3 whereas for other l values $W(l) \approx -1/3 \times 1/3 = -1/9$] yielding $S(k) \approx \delta_{k,2\pi/3} N/9$. Furthermore (in Fig. 2), the peak of the structure factor $S(Q)$ (which remains essentially constant at all relevant interactions $V_2 > 10$) rapidly decreases as n decreases from $1/3$—a trend that is similar to that of $S(Q)$ for the t-V model as one moves away from half-filling.[59] Nevertheless, the plots of correlation function (in Fig. 3) do not seem to decay at large distance (for both $n = 1/4$ and $n = 1/5$) while the structure factor peak (for $n = 1/4$) seems to grow monotonically with system size—all indicative of a CDW. Later on, the above ambivalence will be resolved and it will be demonstrated unequivocally that our
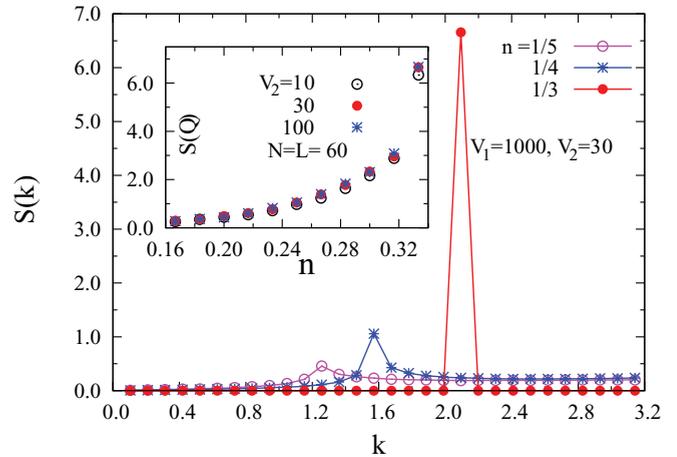
FIG. 2. (Color online) WQMC plot of the structure factor $S(k)$ versus k—for $N = L = 60$, $\beta = L\Delta\tau$ with $\Delta\tau = 0.125$, and at various densities—shows CDW at $n = 1/3$ with $S(Q) \approx N/9$, i.e., maximum allowed value. The peak values $S(Q)$ rapidly fall as n moves away from $1/3$ and are independent of V_2 at large values of V_2 (see inset).

t-V_1-V_2 model has a CDW only at $n = 1/3$, while at other fillings $n < 1/3$ superfluidity (and no CDW) results.

Since $V_1 = \infty$ and because we are dealing with a one-dimensional system, we simplify the phase transition analysis by performing an exact mapping of the N-site t-V_1-V_2 model onto a t-V model with $N - N_p$ sites and with $V = V_2$. This enables us to access bigger system sizes for performing numerics; furthermore, since the phase diagram of the t-V model is well known, we can clearly determine the existence of a CDW which was not possible using the above structure-factor/correlation-function analysis. Later, we will also show that the t-V model lends itself to a simple finite size scaling approach for obtaining accurately the superfluid density in the thermodynamic limit.

We first recognize that we can recast the HCB Hamiltonian in Eq. (16) as the following projected Hamiltonian H_b^P where
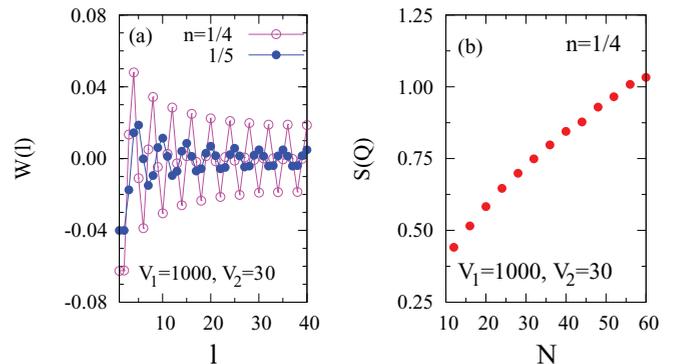
FIG. 3. (Color online) Plots, obtained using WQMC at $\beta = N\Delta\tau$ with $\Delta\tau = 0.125$, showing correlations in the t-V_1-V_2 model. The correlation function $W(l)$, plotted for $N = 80$ sites in (a), does not seem to decay. The peak of the structure factor $S(Q)$, plotted in (b) for various system sizes at $n = 1/4$, grows monotonically.

NN sites of a particle are projected out:

$$H_b^P = \sum_j [-T\{(1 - n_{j-1})b_j^\dagger b_{j+1}(1 - n_{j+2}) + \text{H.c.}\}$$

$$+ V_2(1 - n_{j-1})n_j(1 - n_{j+1})n_{j+2}(1 - n_{j+3})]$$

$$= \sum_j [-T(\tilde{b}_j^\dagger \tilde{b}_{j+1} + \text{H.c.}) + V_2 \tilde{n}_j \tilde{n}_{j+2}], \quad (17)$$

where $\tilde{b}_j^\dagger \equiv (1 - n_{j-1})b_j^\dagger(1 - n_{j+1})$ and $\tilde{n}_j \equiv \tilde{b}_j^\dagger \tilde{b}_j$. Next, we observe that H_b^P commutes with $\sum_j n_j(1 - n_{j+1})$ and thus the total number of excitons (with each exciton comprised of a particle with a hole to its right) is conserved. Physically, this is due to the fact that infinite NN repulsion ensures that the neighboring sites of a particle are unoccupied. With each particle, we associate only one neighboring vacant site (say, the site on the right side of the particle) so that situations such as particles on NNN sites can also be dealt with. Then by deleting the sites of the holes in all the excitons and having only a NN interaction $V = V_2$ and no other interaction in the reduced system of $N_1 \equiv N - N_p$ sites, we get the same eigenenergies (see Ref. 60 for a similar analysis for the t-V model in one-dimension). We further recognize that there is a one-to-one mapping between the eigenstates of the H_b^P Hamiltonian and the eigenstates of the t-V Hamiltonian $H_{t\text{-}V}$,

$$H_{t\text{-}V} = \sum_j [-T(b_j^\dagger b_{j+1} + \text{H.c.}) + V n_j n_{j+1}], \quad (18)$$

with $V = V_2$ and N_1 sites while the corresponding eigenenergies are identical. We can thus extract the eigenenergy spectrum of the t-V_1-V_2 model by studying the equivalent t-V model. We first observe that $n = N_p/N = 1/3$ for the t-V_1-V_2 model corresponds to the $n = N_p/(N - N_p) = 1/2$ for the t-V model and thus superfluid density vanishes (as the two models have the same eigenenergies) and a CDW results[59] since the mass gap is the same for both. Furthermore, at all fractions $n < 1/3$ for the t-V_1-V_2 model we get a superfluid (and no CDW) since for the t-V model the same is true at $n < 1/2$.[59] Lastly, since $n = 1$ for the t-V model translates to $n = 1/2$ for the t-V_1-V_2 model, we note that electron-hole symmetry for the t-V model guarantees that t-V_1-V_2 model exhibits superfluidity and absence of CDW for $1/3 < n < 1/2$ as well.

V. SUPERFLUID DENSITY

We will now substantiate the above observations on the occurrence of superfluidity through calculating the superfluid density by threading the chain with an infinitesimal magnetic flux. We will exploit the one-dimensionality of the system and outline a simple finite size scaling approach to calculate the superfluid density in the thermodynamic limit. We first note that the energy for the t-V_1-V_2 model, when $V_2 = \infty$ and (as before) $V_1 = \infty$, is given by the tight binding Hamiltonian energy for $N_2 \equiv N - 2N_p$ particles where we have excluded both the NN and NNN holes to the right of the particles in the t-V_1-V_2 model. The total energy, when threaded by a flux θ, is expressed as

$$E(\theta) = -2T \sum_k \cos[k + \theta/N_2]. \quad (19)$$
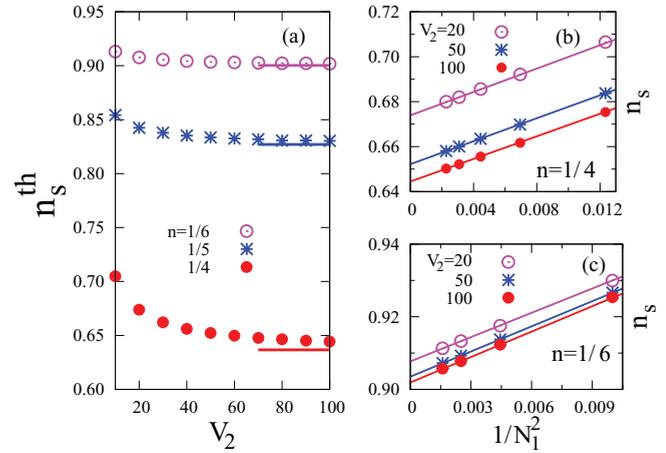
FIG. 4. (Color online) Superfluid density for an infinite system n_s^{th} at various densities n and interactions V_2 for the t-V_1-V_2 model at $V_1 = \infty$ are depicted in (a). Values of n_s^{th} in (a) are the intercepts, obtained by extrapolation of the straight lines through the n_s data plotted at various $1/N_1^2$ values, in figures such as (b) and (c). The solid lines in (a) are for $V_2 = \infty$ and obtained from Eq. (20).

Then the superfluid fraction is given by[61,62]

$$n_s = \frac{N_2^2}{N_p T}\left[\frac{1}{2}\frac{\partial^2 E}{\partial \theta^2}\right]_{\theta=0} = \frac{1}{N_p}\frac{\sin\left(\frac{\pi N_p}{N_2}\right)}{\sin\left(\frac{\pi}{N_2}\right)}, \quad (20)$$

where antiperiodic (periodic) boundary conditions have been taken for even (odd) values of N_p. The superfluid density in the thermodynamic limit n_s^{th} can be related to the finite (N_2-site) system superfluid density n_s as follows:

$$n_s^{\text{th}} = n_s\left[1 - \frac{1}{6}\left(\frac{\pi}{N_2}\right)^2 + \frac{1}{120}\left(\frac{\pi}{N_2}\right)^4 \cdots\right]. \quad (21)$$

From the above expression (valid for $V_2 = \infty$), at a fixed density, we expect $(n_s^{\text{th}} - n_s)/n_s \propto 1/N_2^2$ or $1/N_1^2$ (with corrections of order $1/N_2^4$ or $1/N_1^4$) for the large but finite V_2 case as well. We calculated the superfluid density at various large values of V_2, system sizes N, and filling fractions n; we find [as exemplified in Figs. 4(b) and 4(c)] that n_s indeed varies linearly with $1/N_1^2$, using which we obtain the various n_s^{th} values.

From Fig. 4(a), we see that the superfluid density (plotted in the thermodynamic limit) gradually decreases with increasing V_2 and reaches the asymptotic value; the n_s^{th} values for smaller filling fractions decrease more slowly because repulsion is less effective at lower densities. Regarding the superfluid density at $n = 1/3$ and $V_2 = \infty$, it vanishes at all system sizes as can be seen from Eq. (20). However, at finite $V_2 \geqslant 10$, n_s vanishes exponentially with system size [as shown in Fig. (5)] which is consistent with the fact that there is a full CDW gap at $n = 1/3$.

VI. BEC OCCUPATION NUMBER

Lastly, we will calculate the Bose-Einstein condensate (BEC) occupation number n_0. We first recall the well-established result that n_0, for a system of HCB in a one-dimensional tight binding lattice, varies as $C(n)\sqrt{N}$ in the
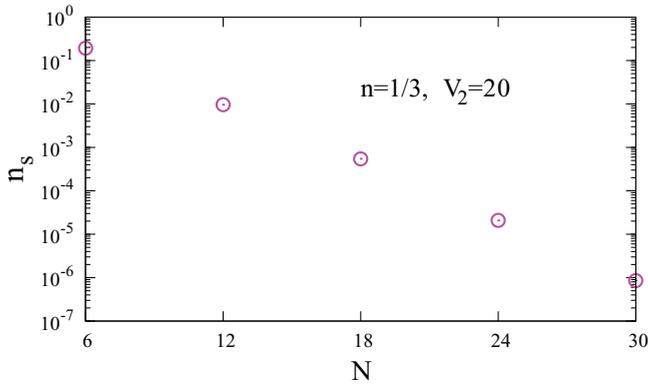
FIG. 5. (Color online) Superfluid density decaying exponentially with system size for the CDW state at one-third filling and large NNN repulsion V_2.

thermodynamic limit with the coefficient $C(n)$ monotonically increasing from 0 as the density n increases from 0 to $1/2$;[63,64] consequently, the condensate fraction $n_0/N_p \propto 1/\sqrt{N} \to 0$. Next, in the presence of repulsion (as argued below), we expect the BEC occupation number n_0 to again scale as $\sqrt{N}$; however, the coefficient of $\sqrt{N}$ will be smaller due to the restriction on hopping imposed by repulsion.

The Bose-Einstein condensate (BEC) occupation number n_0 is obtained from

$$n_0 = \frac{1}{N}\sum_{i,j}\langle\Psi_0|b_i^\dagger b_j|\Psi_0\rangle, \qquad (22)$$

where $|\Psi_0\rangle$ is the ground state. We calculate n_0 using two methods: modified Lanczos for smaller systems and a newly developed WQMC method for both small and larger systems (see Fig. 6). The values of n_0 for our t-V_1-V_2 model in a N-site original system S_O at various densities [such as
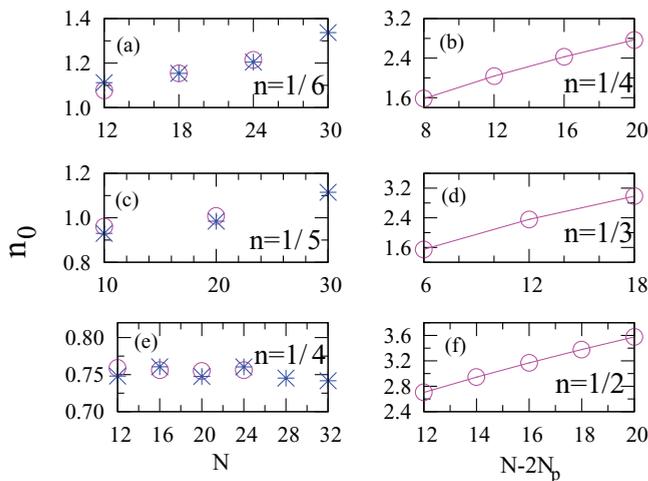
FIG. 6. (Color online) Plots of BEC occupation number n_0, obtained from modified Lanczos (open circles) and WQMC (crosses), with (a), (c), and (e) pertaining to the t-V_1-V_2 model (with $V_1 = \infty$, and $V_2 = 35$) while (b), (d), and (f) respectively pertain to the corresponding tight binding model with enhanced densities $N_p/(N - 2N_p)$. For WQMC, $\beta = N\Delta\tau$ with $\Delta\tau = 0.125, 0.15$, and 0.175 for (a), (c), and (e), respectively.

$n = 1/4, 1/5, 1/6$] seem to be smaller than the n_0 for the corresponding transformed tight binding system S_{2N_p}, realized when $V_1 = V_2 = \infty$, with $N - 2N_p$ sites and enhanced densities $[n/(1 - 2n) = 1/2, 1/3, 1/4$, respectively]. This can be understood from the fact that, in the transformed S_{2N_p} system of $N - 2N_p$ sites [based on Eq. (22)], a particle can hop to more sites between two particles than in the original t-V_1-V_2 system leading to a larger n_0. For the S_{2N_p} system, it is important to realize that $n_0 \propto \sqrt{N - 2N_p} \propto \sqrt{N}$.

We will now consider a tight binding system S_{4N_p} with $N - 4N_p$ sites and N_p particles so as to obtain the lower bound for the BEC occupation number n_0 for the N-site t-V_1-V_2 system S_O. For every configuration in the S_{4N_p} system, there is a corresponding configuration in the S_O system that can be obtained by adding two empty sites to the right and two empty sites to the left of all particles. Furthermore, the ground state kinetic energy contribution of the S_{4N_p} and S_{2N_p} systems are both proportional to N; hence, in the ground state of the original S_O system, the combined probability weighting of all the configurations obtained from the S_{4N_p} system (by adding four empty sites next to every particle) is a finite fraction. Since the BEC occupation number n_0 of the S_{4N_p} system scales as $\sqrt{N}$, it follows that the lower bound of the n_0 for the original S_O system also varies as $\sqrt{N}$. Thus, the BEC occupation number n_0 of the original N-site t-V_1-V_2 system S_O will vary as $\sqrt{N}$ since it is constrained from above by $n_0 \propto \sqrt{N}$ for the S_{2N_p} system.

At higher densities (i.e., $1/3 > n \geqslant 1/5$) in our t-V_1-V_2 model, we find that the values of n_0 seem to increase more slowly with system size [see Figs. 6(a), 6(c), and 6(e)]—this being due to smaller coefficients of $\sqrt{N}$ resulting from interaction effects. Moreover, we also note [from Figs. 6(b) and 6(e)] that the value of n_0 [i.e., the coefficient of $\sqrt{N}$ in the expression for n_0] decreases due to repulsion.

Our WQMC method (see Appendix B for details) to obtain BEC fraction is a modification of the standard approach to studying correlations in the xxz model.[58,65] Since the Hamiltonian is real, it can be shown that the probability amplitude of any basis state in the ground state expression can be taken as real and non-negative. Consequently, we approximate the ground state by

$$|\Psi\rangle = \sum_i \sqrt{\frac{\langle\phi_i|\exp[-\beta H]|\phi_i\rangle}{Z}}|\phi_i\rangle, \qquad (23)$$

with Z being the partition function, $|\phi_i\rangle$ a basis state of the system in the occupation number representation, and β being sufficiently large. Then we calculate n_0 by setting $|\Psi_0\rangle = |\Psi\rangle$ in Eq. (22). Our WQMC approach to n_0 has been benchmarked against the modified Lanczos method for small system sizes (see Fig. 6). The number of passes needed to estimate $|\Psi\rangle$ turns out to be an order of magnitude larger than that needed for obtaining correlation functions by WQMC. We take $|\Psi\rangle$ to be the state that produces an estimate of the kinetic energy $\langle\Psi|K|\Psi\rangle$ (with K being the kinetic energy operator) that is closest to the usual WQMC estimate $\langle\langle\phi_i|\exp[-\beta H]K|\phi_i\rangle/\langle\phi_i|\exp[-\beta H]|\phi_i\rangle\rangle_{\text{QMC}}$ where $\langle\rangle_{\text{QMC}}$ denotes a quantum Monte Carlo average over various states $|\phi_i\rangle$.

VII. CONCLUSIONS

In this paper, we have analyzed the correlated NN singlet phase predicted by the effective Hamiltonian of the Hubbard-Holstein model by essentially mapping the Hamiltonian onto the well-understood one-dimensional t-V model with large repulsion. Because the physics is dictated by the t-V model, we find that CDW and superfluidity occur mutually exclusively with CDW resulting only at $n = 1/3$ while superfluidity manifests itself at all other fillings. We also show that the BEC occupation number n_0 for our model scales as $\sqrt{N}$ similar to the n_0 for a HCB tight binding model; additionally, we demonstrate numerically (using our WQMC method and a modified Lanczos algorithm), at $n \neq 1/3$, that the n_0 for our model is smaller than the n_0 for a HCB tight binding model.

We close by observing that, while CDW and superconductivity seem to be incompatible in the one-dimensional HHM, experimental results (such as those reported in Refs. 1–3) suggest that they can coexist in higher dimensions. Furthermore, the vanishing of BEC fraction for the HHM is again an artifact of the one-dimensionality and should make way to nonzero fractions for higher dimensions just as in the case of the xxz model.[62]

ACKNOWLEDGMENTS

APPENDIX A

In this Appendix, we will outline our approach to carrying out perturbation theory and obtaining the ground state energy. We assume a Hamiltonian of the form $H = H_0 + H_1$ where the unperturbed H_0 has separable eigenstates $|n,m\rangle = |n\rangle_{\text{el}} \otimes |m\rangle_{ph}$ with $|0,0\rangle$ being the ground state with zero phonons; the eigenenergies, corresponding to $|n,m\rangle$, are $E_{n,m}^{(0)} = E_n^{\text{el}} + E_m^{\text{ph}}$. Furthermore, the perturbation H_1 is the electron-phonon interaction term of the form given in Eq. (7).

After a canonical transformation,[15] we obtain

$$\tilde{H} = e^S H e^{-S} = H_0 + H_1 + [H_0 + H_1, S] + \tfrac{1}{2}[[H_0 + H_1, S], S]. \tag{A1}$$

In the ground state energy, we know that the first-order perturbation term is zero by construction (in fact, $\langle n_1, 0|H_1|n_2, 0\rangle = 0$). To eliminate the first-order term in H_1, we set $H_1 + [H_0, S] = 0$. Consequently, we obtain the matrix elements

$$\langle n_1, m_1|S|n_2, m_2\rangle = -\frac{\langle n_1, m_1|H_1|n_2, m_2\rangle}{(E_{n_1, m_1} - E_{n_2, m_2})}. \tag{A2}$$

We now assume that both NN hopping integral $t e^{-g^2}$ and the Heisenberg spin interaction strength J are much smaller compared to the phononic energy ω_0 which is true at large couplings g. Hence, we make the approximation $(E_{n_1, m_1}^{(0)} - E_{n_2, m_2}^{(0)}) \simeq (E_{m_1}^{\text{ph}} - E_{m_2}^{\text{ph}})$; then, using Eqs. (A1) and (A2), we

obtain

$$_{\text{ph}}\langle m_1|\tilde{H}|m_2\rangle_{\text{ph}} \simeq {}_{\text{ph}}\langle m_1|H_0|m_2\rangle_{\text{ph}}$$
$$+ \frac{1}{2}\sum_{\bar{m}} {}_{\text{ph}}\langle m_1|H_1|\bar{m}\rangle_{\text{ph ph}}\langle\bar{m}|H_1|m_2\rangle_{\text{ph}}$$
$$\times\left[\frac{1}{E_{m_2}^{\text{ph}} - E_{\bar{m}}^{\text{ph}}} + \frac{1}{E_{m_1}^{\text{ph}} - E_{\bar{m}}^{\text{ph}}}\right]. \tag{A3}$$

Next, it is important to note that the second order correction $E_{n,m}^{(2)}$, corresponding to the unperturbed eigenenergy $E_{n,m}^{(0)}$, can be expressed as follows:

$$E_{n,m}^{(2)} = \sum_{\bar{m}} \frac{\langle n,m|H_1|\bar{m}\rangle_{\text{ph ph}}\langle\bar{m}|H_1|n,m\rangle}{E_m^{\text{ph}} - E_{\bar{m}}^{\text{ph}}}$$
$$\simeq \langle n,m|\tilde{H}|n,m\rangle - \langle n,m|H_0|n,m\rangle. \tag{A4}$$

Furthermore, since $\langle n_1, 0|H_1|n_2, 0\rangle = 0$, $\langle n,0|\tilde{H}|n,0\rangle$ is the total energy that resulted from performing second order perturbation theory on the unperturbed energy $E_{n,0}^{(0)}$. Our procedure for finding ground state amounts to obtaining the lowest eigenvalue for the matrix with elements $\langle n_1, 0|\tilde{H}|n_2, 0\rangle$; this is equivalent to finding the ground state of the effective Hamiltonian H_e (as was done in Ref. 15):

$$H_e = {}_{\text{ph}}\langle 0|H_0|0\rangle_{\text{ph}} + H^{(2)}, \tag{A5}$$

where

$$H^{(2)} = \sum_{\bar{m}} \frac{_{\text{ph}}\langle 0|H_1|\bar{m}\rangle_{\text{ph}} \times {}_{\text{ph}}\langle\bar{m}|H_1|0\rangle_{\text{ph}}}{E_0^{\text{ph}} - E_{\bar{m}}^{\text{ph}}}. \tag{A6}$$

This procedure amounts to considering the restricted subspace spanned by eigenstates $|n,0\rangle_1$ obtained from carrying out first order perturbation theory on $|n,0\rangle$:

$$|n,0\rangle_1 = |n,0\rangle + \sum_{\bar{m}} \frac{|\bar{m}\rangle_{\text{ph ph}}\langle\bar{m}|H_1|n,0\rangle}{E_0^{\text{ph}} - E_{\bar{m}}^{\text{ph}}}. \tag{A7}$$

It is important to recognize that the state $|n,0\rangle_1$ is not separable, i.e., cannot be expressed as a product of an electronic wave function and a phononic wave function. We have restricted ourselves to the subspace of the states $|n,0\rangle_1$ because the states $|n,m \neq 0\rangle_1$ correspond to higher energy states due to the fact that the electronic excitation energy is much smaller than the phononic energy, i.e., $t e^{-g^2} \ll \omega_0$. Additionally, we would like to point out that the total ground state energy (in second order perturbation theory) is obtained by diagonalizing the matrix whose elements are $\langle n_1, 0|H|n_2, 0\rangle_1$.

APPENDIX B: WQMC FOR BEC FRACTION

We will discuss, in brief, the usual world-line quantum Monte Carlo (WQMC) approach[58,65] adapted for calculating correlations in our t-V_1-V_2 model Hamiltonian given below:

$$H_b = \sum_j H^j = \sum_j [-T(b_j^\dagger b_{j+1} + \text{H.c.}) + V_1 n_j n_{j+1} + V_2 n_j n_{j+2}]. \tag{B1}$$

Since this is quite similar to the t-V model, we can employ the checkerboard decomposition $H_b = H_1 + H_2$ where $H_1 = \sum_{j\text{ odd}} H^j$ and $H_2 = \sum_{j\text{ even}} H^j$. It is important to note that both H_1 and H_2 consist of independent two-site pieces.

Because of the decomposition, it becomes easier to evaluate the expectation value of an operator A given by

$$\langle A \rangle = \frac{\text{Tr}[Ae^{-\beta H_b}]}{\text{Tr}[e^{-\beta H_b}]}, \tag{B2}$$

with A involving only number operators (such as $n_i n_j$) or NN hopping operators (such as $b_j^\dagger b_{j+1} + \text{H.c.}$). Now we calculate the partition function:

$$Z = \text{Tr}[e^{-\beta H_b}]$$
$$= \sum_{i_1,\dots,i_{2L}} \langle i_1|U_1|i_{2L}\rangle\langle i_{2L}|U_2|i_{2L-1}\rangle\dots\langle i_3|U_1|i_2\rangle\langle i_2|U_2|i_1\rangle.$$

Here $U_i = e^{-\Delta\tau H_i}$, $\beta = L\Delta\tau$, and each of $|i_1\rangle,\dots,|i_{2L}\rangle$ form a complete basis set in the occupation number representation. Here the world lines are the locus of the particles in the imaginary time (τ) direction.

For the density-density correlation function $\langle n_i n_{i+l}\rangle$ (which is the expectation value of a diagonal operator), the above procedure of inserting $2L$ time slices yields the simple form

$$\langle n_i n_{i+l}\rangle = \tfrac{1}{2}\langle [\langle i_L|n_i n_{i+l}|i_L\rangle + \langle i_{L+1}|n_i n_{i+l}|i_{L+1}\rangle]\rangle_{\text{QMC}},$$

where $\langle\;\;\rangle_{\text{QMC}}$ represents the average over many QMC passes. Notice that we have concentrated only on L and $L+1$ time slice indexes although expectation value can be taken over all the $2L$ time slice indexes for better statistics. As for $\langle b_j^\dagger b_{j+1} + \text{H.c.}\rangle$ (which corresponds to a nondiagonal operator), WQMC procedure yields

$$\langle b_j^\dagger b_{j+1} + \text{H.c.}\rangle = \left\langle \frac{\langle i_M|(b_j^\dagger b_{j+1} + \text{H.c.})U_k|i_{M+1}\rangle}{\langle i_M|U_k|i_{M+1}\rangle}\right\rangle_{\text{QMC}},$$

where, for odd (even) values of j, we take $k = 1$ (2) and even (odd) M. However, as regards obtaining the expectation value of $(b_j^\dagger b_{j+m} + \text{H.c.})$ for $m > 1$, the simple procedure (involving checkerboard decomposition) given above is not applicable; moreover, other suggested procedures in the literature are complicated.[58]

Here, we propose an alternate simple method for evaluating $\langle b_j^\dagger b_{j+m} + \text{H.c.}\rangle$ for $m > 1$ and thus obtaining the BEC occupation number

$$n_0 = \frac{1}{N}\sum_{i,j}\langle\Psi_0|b_i^\dagger b_j|\Psi_0\rangle, \tag{B3}$$

with $|\Psi_0\rangle$ being the ground state. To the WQMC method mentioned above, we add our trick to construct $|\Psi_0\rangle$ as a linear combination of the basis states $|\phi_i\rangle$ in the occupation number representation, i.e., $|\Psi_0\rangle = \sum_i a_i|\phi_i\rangle$ with $\sum_i a_i^2 = 1$. Once we get a good estimate of the ground state $|\Psi_0\rangle$, we can calculate the expectation values of any operator.

After equilibrium (which is attained after several QMC passes), we run the simulation for a sufficient number of QMC passes and store the basis states corresponding to time slices L and $L+1$ in each pass. It is obvious that some of the basis states will occur more frequently. The frequency of occurrence of a basis state $|\phi_i\rangle$ is proportional to the probability (a_i^2) of its occurrence in the expansion of the ground state $|\Psi_0\rangle$. Now, the coefficients a_i can be taken as real because the Hamiltonian is real and consequently $|\Psi_0\rangle$ can also be taken as real. Furthermore, all a_i can be taken to be positive for the following reason. Firstly, the expectation values of NN and NNN interaction terms remain unaffected by the sign of a_i. Next, the expectation value of the hopping term is given by

$$-T\langle\Psi_0|b_l^\dagger b_{l+1}|\Psi_0\rangle = -T\sum_{i,j}\langle\phi_i|a_i(b_l^\dagger b_{l+1})a_j|\phi_j\rangle]$$
$$= -T\sum_{i,k}\langle\phi_i|a_i c_k|\phi_k\rangle] = -T\sum_i a_i c_i. \tag{B4}$$

This value is minimized when a_i and c_i have the same sign. Then, if we take a_i to be positive for all i, $c_i > 0$ for all i. Thus in $|\Psi_0\rangle = \sum_i a_i|\phi_i\rangle$, we can take all a_i to be positive and real.

Let $|\Psi_i\rangle$ and E_i be the eigenstates and the eigenenergies of the Hamiltonian with E_0 being the ground state energy. For sufficiently large β, we approximate the ground state by

$$|\Psi\rangle = \sum_i \sqrt{\frac{\langle\phi_i|\exp[-\beta H]|\phi_i\rangle}{Z}}|\phi_i\rangle, \tag{B5}$$

because then

$$|\Psi\rangle = \sum_i \sqrt{\frac{\langle\phi_i|\sum_j|\Psi_j\rangle\langle\Psi_j|\exp[-\beta H]\sum_k|\Psi_k\rangle\langle\Psi_k||\phi_i\rangle}{Z}}|\phi_i\rangle$$
$$\approx \sum_i \sqrt{\frac{\langle\phi_i|\Psi_0\rangle\exp[-\beta E_0]\langle\Psi_0|\phi_i\rangle}{Z}}|\phi_i\rangle$$
$$\approx \sum_i \langle\phi_i|\Psi_0\rangle|\phi_i\rangle = |\Psi_0\rangle, \tag{B6}$$

since the partition function $Z = \sum_i\langle\Psi_i|\exp[-\beta H]|\Psi_i\rangle \approx \exp[-\beta E_0]$.

---

[1]For a review, see R. L. Withers and J. A. Wilson, J. Phys. C **19**, 4809 (1986).

[2]E. Kim and M. H. W. Chan, Nature (London) **427**, 225 (2004); Science **305**, 1941 (2004).

[3]S. H. Blanton, R. T. Collins, K. H. Kelleher, L. D. Rotter, Z. Schlesinger, D. G. Hinks, and Y. Zheng, Phys. Rev. B **47**, 996 (1993).

[4]W. W. Fuller, P. M. Chaikin, and N. P. Ong, Phys. Rev. B **24**, 1333 (1981).

[5]A. Rusydi, W. Ku, B. Schulz, R. Rauer, I. Mahns, D. Qi, X. Gao, A. T. S. Wee, P. Abbamonte, H. Eisaki, Y. Fujimaki, S. Uchida, and M. Rübhausen, Phys. Rev. Lett. **105**, 026402 (2010); P. Abbamonte, G. Blumberg, A. Rusydi, A. Gozar, P. G. Evans, T. Siegrist, L. Venema, H. Eisaki, E. D. Isaacs, and G. A. Sawatzky, Nature (London) **431**, 1078 (2004).

[6]H. Mori, I. Hirabayashi, S. Tanaka, T. Mori, Y. Maruyama, and H. Inokuchi, Solid State Commun. **80**, 411 (1991).

[7]J. Merino and R. H. McKenzie, Phys. Rev. Lett. **87**, 237002 (2001).

[8] K. Kudo, Y. Nishikubo, and M. Nohara, J. Phys. Soc. Jpn. **79**, 123710 (2010).

[9] A. Lanzara, P. V. Bogdanov, X. J. Zhou, S. A. Kellar, D. L. Feng, E. D. Lu, T. Yoshida, H. Eisaki, A. Fujimori, K. Kishio, J.-I. Shimoyama, T. Noda, S. Uchida, Z. Hussain, and Z. X. Shen, Nature (London) **412**, 510 (2001).

[10] G.-H. Gweon, T. Sasagawa, S. Y. Zhou, J. Graf, H. Takagi, D.-H. Lee, and A. Lanzara, Nature (London) **430**, 187 (2004).

[11] A. Lanzara, N. L. Saini, M. Brunelli, F. Natali, A. Bianconi, P. G. Radaelli, and S.-W. Cheong, Phys. Rev. Lett. **81**, 878 (1998).

[12] A. J. Millis, P. B. Littlewood, and B. I. Shraiman, Phys. Rev. Lett. **74**, 5144 (1995).

[13] F. Massee, S. de Jong, Y. Huang, W. K. Siu, I. Santoso, A. Mans, A. T. Boothroyd, D. Prabhakaran, R. Follath, A. Varykhalov, L. Patthey, M. Shi, J. B. Goedkoop, and M. S. Golden, Nat. Phys. **7**, 978 (2011).

[14] O. Gunnarsson, Rev. Mod. Phys. **69**, 575 (1997).

[15] S. Reja, S. Yarlagadda, and P. B. Littlewood, Phys. Rev. B **84**, 085127 (2011).

[16] A. Dobry, A. Greco, J. Lorenzana, and J. Riera, Phys. Rev. B **49**, 505 (1994).

[17] A. Dobry, A. Greco, J. Lorenzana, J. Riera, and H. T. Diep, Europhys. Lett. **27**, 617 (1994).

[18] B. Bäuml, G. Wellein, and H. Fehske, Phys. Rev. B **58**, 3663 (1998).

[19] M. Tezuka, R. Arita, and H. Aoki, Phys. Rev. B **76**, 155114 (2007).

[20] Shigetoshi Sota and Takami Tohyama, Phys. Rev. B **82**, 195130 (2010).

[21] J. E. Hirsch and E. Fradkin, Phys. Rev. B **27**, 4302 (1983).

[22] J. E. Hirsch, Phys. Rev. B **31**, 6022 (1985).

[23] E. Berger, P. Valášek, and W. von der Linden, Phys. Rev. B **52**, 4806 (1995).

[24] Z. B. Huang, W. Hanke, E. Arrigoni, and D. J. Scalapino, Phys. Rev. B **68**, 220507(R) (2003).

[25] R. P. Hardikar and R. T. Clay, Phys. Rev. B **75**, 245103 (2007).

[26] A. Macridin, G. A. Sawatzky, and M. Jarrell, Phys. Rev. B **69**, 245111 (2004).

[27] M. Grilli and C. Castellani, Phys. Rev. B **50**, 16880 (1994).

[28] J. Keller, C. E. Leal, and F. Forsthofer, Physica B **206-207**, 739 (1995).

[29] E. Koch and R. Zeyher, Phys. Rev. B **70**, 094510 (2004).

[30] U. Trapper, H. Fehske, M. Deeg, and H. Buttner, Z. Phys. B: Condens. Matter **93**, 465 (1994).

[31] C. A. Perroni, V. Cataudella, G. De Filippis, and V. Marigliano Ramaglia, Phys. Rev. B **71**, 113107 (2005).

[32] J. K. Freericks and M. Jarrell, Phys. Rev. Lett. **75**, 2570 (1995).

[33] M. Capone, G. Sangiovanni, C. Castellani, C. Di Castro, and M. Grilli, Phys. Rev. Lett. **92**, 106401 (2004).

[34] W. Koller, D. Meyer, Y. Ōno, and A. C. Hewson, Europhys. Lett. **66**, 559 (2004).

[35] W. Koller, D. Meyer, and A. C. Hewson, Phys. Rev. B **70**, 155103 (2004).

[36] G. S. Jeon, T.-H. Park, J. H. Han, H. C. Lee, and H.-Y. Choi, Phys. Rev. B **70**, 125114 (2004).

[37] G. Sangiovanni, M. Capone, C. Castellani, and M. Grilli, Phys. Rev. Lett. **94**, 026401 (2005).

[38] G. Sangiovanni, M. Capone, and C. Castellani, Phys. Rev. B **73**, 165123 (2006).

[39] J. Bauer and A. C. Hewson, Phys. Rev. B **81**, 235113 (2010).

[40] Johannes Bauer and Giorgio Sangiovanni, Phys. Rev. B **82**, 184535 (2010).

[41] R. Zeyher and M. L. Kulić, Phys. Rev. B **53**, 2850 (1996).

[42] Y. Takada and A. Chatterjee, Phys. Rev. B **67**, 081102 (2003).

[43] H. Fehske, D. Ihle, J. Loos, U. Trapper, and H. Buttner, Z. Phys. B: Condens. Matter **94**, 91 (1994).

[44] A. Di Ciolo, J. Lorenzana, M. Grilli, and G. Seibold, Phys. Rev. B **79**, 085101 (2009).

[45] P. Barone, R. Raimondi, M. Capone, C. Castellani, and M. Fabrizio, Phys. Rev. B **77**, 235115 (2008).

[46] Alexandre Payeur and David Sénéchal, Phys. Rev. B **83**, 033104 (2011).

[47] E. R. Gagliano, E. Dagotto, A. Moreo, and F. C. Alcaraz, Phys. Rev. B **34**, 1677 (1986); **35**, 5297 (1987).

[48] A. S. Alexandrov and N. F. Mott, *Polarons and Bipolarons* (World Scientific, Singapore, 1995).

[49] E. V. L. de Mello and J. Ranninger, Phys. Rev. B **58**, 9098 (1998); B. K. Chakraverty, J. Ranninger, and D. Feinberg, Phys. Rev. Lett. **81**, 433 (1998).

[50] R. T. Clay and R. P. Hardikar Phys. Rev. Lett. **95**, 096401 (2005); R. P. Hardikar and R. T. Clay, Phys. Rev. B **75**, 245103 (2007).

[51] J. Bonča, T. Katrašnik, and S. A. Trugman, Phys. Rev. Lett. **84**, 3153 (2000).

[52] H. Eskes and R. Eder, Phys. Rev. B **54**, 14226 (1996).

[53] B. Ammon, M. Troyer, and H. Tsunetsugu, Phys. Rev. B **52**, 629 (1995).

[54] A. P. Balachandran, E. Ercolessi, G. Morandi, and A. M. Srivastava, Int. J. Mod. Phys. B **4**, 2057 (1990).

[55] I. G. Lang and Yu. A. Firsov, Zh. Eksp. Teor. Fiz. **43**, 1843 (1962) [Sov. Phys. JETP **16**, 1301 (1963)].

[56] R. Pankaj and S. Yarlagadda, arXiv:1203.2327v1.

[57] The phase diagram results for $t/\omega_0 = 0.5$ are qualitatively similar to those for $t/\omega_0 = 1.0$.

[58] R. T. Scalettar, in *Quantum Monte Carlo Methods in Physics and Chemistry*, NATO Science Series, Series C: Mathematical and Physical Sciences Vol. 525, edited by M. P. Nightingale and Cyrus J. Umrigar (Kluwer Academic Publishers, Boston, 1999).

[59] S. Datta, A. Das, and S. Yarlagadda, Phys. Rev. B **71**, 235118 (2005); F. D. M. Haldane, Phys. Rev. Lett. **45**, 1358 (1980).

[60] R. G. Dias, Phys. Rev. B **62**, 7791 (2000).

[61] M. E. Fisher, M. N. Barber, and D. Jasnow, Phys. Rev. A **8**, 1111 (1973).

[62] S. Datta and S. Yarlagadda, Solid State Commun. **150**, 2040 (2010).

[63] A. Lenard, J. Math. Phys. **5**, 930 (1964).

[64] M. Rigol and A. Muramatsu, Phys. Rev. A **72**, 013604 (2005).

[65] J. E. Hirsch, R. L. Sugar, D. J. Scalapino, and R. Blankenbecler, Phys. Rev. B **26**, 5033 (1982).